

Communication

Physicochemical and Antibacterial Evaluation of TiO₂/CNT Mesoporous Nanomaterials Prepared by High-Pressure Hydrothermal Sol–Gel Method under an Ultrasonic Composite Environment

Huansheng Lai ¹, Zilong Zhao ^{2,*}, Wenhe Yu ³, Yuan Lin ⁴ and Zhiyuan Feng ^{2,*} ¹ Sino-French Institute of Nuclear Engineering and Technology, Sun Yat-Sen University, Zhuhai 519082, China² School of Chemical Engineering and Technology, Sun Yat-Sen University, Zhuhai 519082, China³ Beijing Key Laboratory of Materials Utilization of Nonmetallic Minerals and Solid Wastes, National Laboratory of Mineral Materials, Engineering Research Center of Ministry of Education for Geological Carbon Storage and Low Carbon Utilization of Resources, School of Materials Science and Technology, China University of Geosciences, Beijing 100083, China⁴ Technical Center, Taiyuan Iron & Steel (Group) Co., Ltd., Taiyuan 030003, China; linyuan@tisco.com.cn

* Correspondence: zhaozlong@mail.sysu.edu.cn (Z.Z.); fengzhy25@mail.sysu.edu.cn (Z.F.)

Abstract: TiO₂ has attracted significant research interest, principally due to its nontoxicity, high stability, and abundance. Carbon-doped TiO₂ can improve light absorption efficiency. In order to prepare high-efficiency photocatalysts, carbon-doped composites were prepared by hydrothermal reaction in a high-pressure reactor, and then TiO₂/CNT mesoporous composites were prepared by the sol–gel method in an ultrasonic environment. Characterized by SEM and TEM, the composite materials contained TiO₂ nanoparticles as well as CNT. After phase analysis, it was the anatase-doped phase. The following infrared light absorption performance and *Escherichia coli* bactericidal performance tests showed that it had better infrared and visible light absorption performance than pure TiO₂. The TiO₂/CNT mesoporous nanomaterials synthesized in this work are possible for clean industrial productions.

Keywords: carbon nanotubes; TiO₂; mesoporous composite; bactericidal properties



Citation: Lai, H.; Zhao, Z.; Yu, W.; Lin, Y.; Feng, Z. Physicochemical and Antibacterial Evaluation of TiO₂/CNT Mesoporous Nanomaterials Prepared by High-Pressure Hydrothermal Sol–Gel Method under an Ultrasonic Composite Environment. *Molecules* **2023**, *28*, 3190. <https://doi.org/10.3390/molecules28073190>

Academic Editors: Mariana Emilia Ghica, Luciana I. N. Tomé, Ana Dora Rodrigues Pontinha and Andreia Romeiro

Received: 17 March 2023

Revised: 27 March 2023

Accepted: 31 March 2023

Published: 3 April 2023



Copyright: © 2023 by the authors. Licensee MDPI, Basel, Switzerland. This article is an open access article distributed under the terms and conditions of the Creative Commons Attribution (CC BY) license (<https://creativecommons.org/licenses/by/4.0/>).

1. Introduction

With the advent of the steam engine revolution, electrical revolution, and information technology revolution, human beings have advanced by leaps and bounds in intelligent manufacturing, life sciences, and information technology [1–5]. However, with the development of science and technology, human beings also consume a lot of natural resources. In particular, the depletion of fossil non-renewable energy and environmental pollution poses new challenges to the development of science and technology [6–11].

Global climate change has prompted researchers from across the world to work together to search for new technologies for producing clean and renewable energy [12–15]. Photocatalytic reactions on semiconductive TiO₂ are widely used and investigated for (1) water splitting in view of H₂ production and (2) the destruction of environmental pollutants from water and air [16]. Starting from a point of practical engineering application, energy-efficient photocatalysts are highly demanded to effectively utilize the visible light that constitutes 43% of the total sunlight [17]. Hence, it is important to develop a visible light-responsive photo-catalyst, and some efforts have been devoted to developing “second-generation” TiO₂ and other narrow band-gap semiconductors that can absorb visible light [18].

Numerous scientists have made gratifying achievements in the field of semiconductor materials. In particular, the large-scale and low-cost production of titanium dioxide P25

has the advantage of integrating various excellent properties in terms of material activity, specific surface area, and photoelectric performance [19–23]. The discovery of graphene is a gratifying achievement for mankind. The excellent properties of graphene have attracted research by scientists in various fields around the world and have made considerable achievements. However, the manufacturing cost of graphene has always been the bottleneck limiting its development. Therefore, many scientists have conducted research on carbon materials. From diamond and graphite, to fullerenes, carbon nanotubes, etc., carbon materials are full of magic. The development of 3D carbon-based nanocomposite multi-functional membranes has attracted researchers all over the world. The understanding of cavity quantum effect diffusions, reaction/inter-reaction, surface-area-to-volume ratio, and reaction kinetics is still at a preliminary level. Although we are able to produce a 3D nanotube filtration membrane at a thickness of around 200 nm, the further reduction in the thickness of this membrane for the fabrication of the membrane still remains a challenge. Therefore, it is important to search for new materials to fabricate the membrane. It has been reported in the literature that the combination of carbon materials and titanium dioxide can prepare excellent nanocomposite functional materials and exhibit various excellent properties. Especially in the fields of energy and environment, human beings urgently need to find sustainable energy materials and environmental governance materials [18,24–26]. However, the interfacial bonding performance of composite materials has always been a key factor affecting their development, and the composite interface of titanium dioxide and carbon materials in particular has always attracted the research of scientists.

In this paper, the preparation of titanium dioxide nanoparticles coupled with carbon nanotube composites by the high-pressure hydrothermal reaction was studied. Nanomesoporous thin-film materials with a high specific surface area were prepared by the sol–gel method in the environment of ultrasonic radiation. The photoelectric properties and bactericidal properties of the composites were tested. The interface structure of the material was characterized by STEM in order to clarify the interfacial recombination mechanism of titanium dioxide and carbon nanotubes.

2. Experimental Procedure

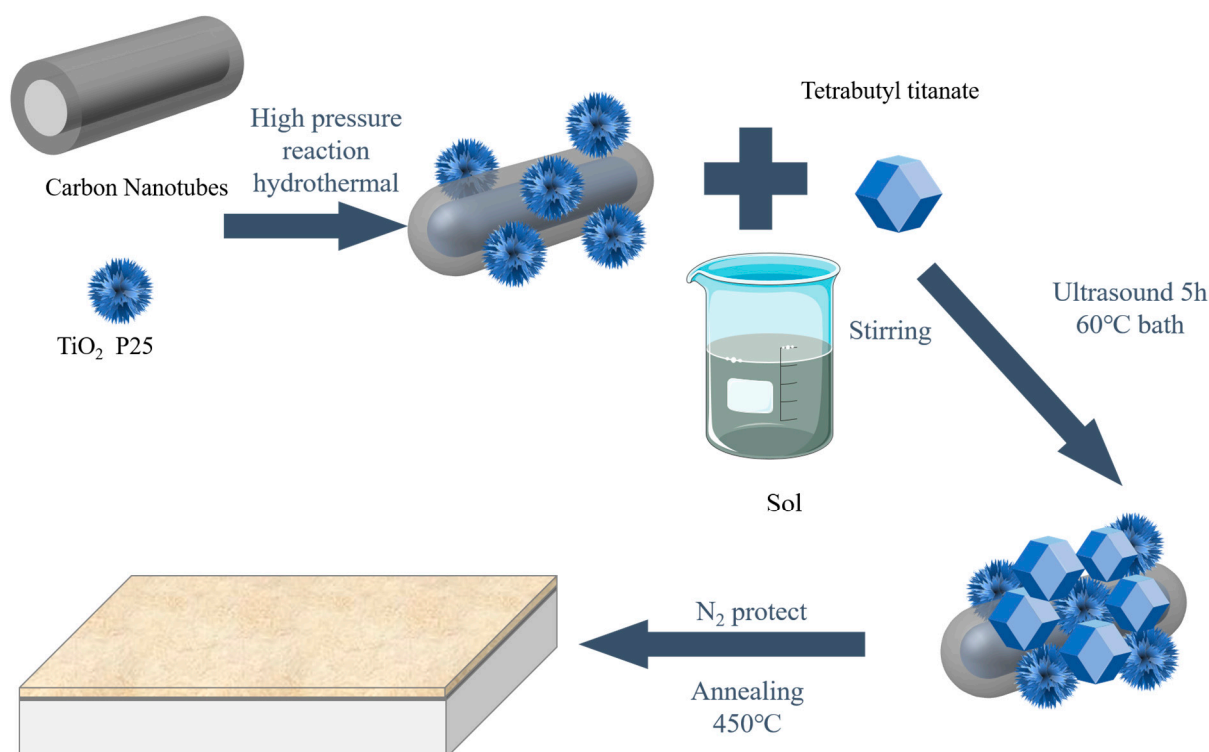
2.1. Materials and Methods

First, commercial P25 TiO₂ particles (InnoCHEM, average particle size = 25 nm) were blended with 5 wt.% multi-wall carbon nanotube (Shanghai, average particle size = 10–20 nm). The carbon-doped composites were prepared by hydrothermal reaction in an autoclave (150 °C, 6 h) using ethanol as solvent. After filtration, the obtained carbon-doped composite was dried in a vacuum drying oven (Jinghong, 80 °C, 2 h).

Tetra-n-butylorthotitanate [Ti(O-i-C₄H₉)₄] (TB) and ethanol absolute (EtOH) were used to prepare the Ti-bases sol. The addition of HCl was added to facilitate the hydrolysis rate of the mixture. The mole ratio of the ingredients was optimized at TB/EtOH = 1:50 with respect to the size of the nanoparticle produced by the sol.

The carbon-doped composite was dispersed into the Ti-based sol at 0.2 g/mL under vigorous magnetic stirring and subsequently placed in the ultrasonic bath for 5 h. The temperature was maintained at 80 °C. The sonicated mixture was then dried overnight at 80 °C and then calcined in an argon furnace (450 °C, 6 h) for converting the amorphous TiO₂ into the anatase phase.

The schematic diagram for material preparation is shown in Scheme 1.



Scheme 1. Schematic illustration of the formation of mesoporous TiO₂/CNT nanomaterials membrane by sol-gel ultrasonic irradiation method.

2.2. Performance and Characterization

Escherichia coli was selected for bactericidal performance. An amount of 10 mg of the sample was added to 10 mL of deionized water (18.2 M Ohm) and sterilized in an automatic high-temperature sterilizer. After 1.15 g/L of the bacterial solution was diluted to 0.01%, 100 μ L was added to TiO₂ sterilization solution and irradiated under 34.4 klux sunlight for 1 h to prepare solid medium (trypsin 10 g, yeast powder 5 g, NaCl 10 g, agar 20 g and deionized water to prepare 1 L solution). Then, the sterilizing solution after illumination was applied to the medium, and the sterilization results were observed after 8 h.

A scanning electron microscope (SEM, JSM-7800F, JEOL, Tokyo, Japan) equipped with an electron backscattered diffraction system was employed for surface characterization. A transmission electron microscope (TEM, JEOL-2100F, Tokyo, Japan) was used for the structural analysis of TiO₂. Phase analysis was carried out on X-ray diffraction (XRD, XPERT-PRO, Hawaii, HI, USA).

3. Results and Discussion

SEM images of the TiO₂ and TiO₂ + CNT mesoporous composite are presented in Figure 1. The TiO₂ prepared by the sol-gel method under ultrasonic irradiation was a mesoporous material (Figure 1a). Carbon nanotubes were rolled sheets of carbon atoms that form cylinders. After adding CNTs, TiO₂ aggregated grow on the surface of carbon fibers and TiO₂ nanoparticles were bonded around CNTs to form nanocomposites (Figure 1b). Moreover, the CNTs were exposed, confirming their successful incorporation into the CNTs. According to the energy dispersive spectroscopy (EDS) mapping in Figure 2. The results confirmed the presence and distribution of C, O, and Ti. The aggregated particles consisted of TiO₂, and the strip structures consisted of CNTs. The green (O)- and yellow (Ti)-colored particles represented the TiO₂ nanoparticles; the red (C)-colored structure represented CNTs. TiO₂ nanoparticles were uniformly distributed on carbon nanotubes, which indicated the bonding between TiO₂ nanoparticles and CNTs. It can be concluded that the one-dimensional CNTs were interlaced to form nanoporous structures, and zero-

dimensional TiO_2 particles were adhered to one-dimensional CNTs through gelation and sintering to form mesoporous composites. The agglomeration of the mesoporous materials was reduced by the ultrasonic process.

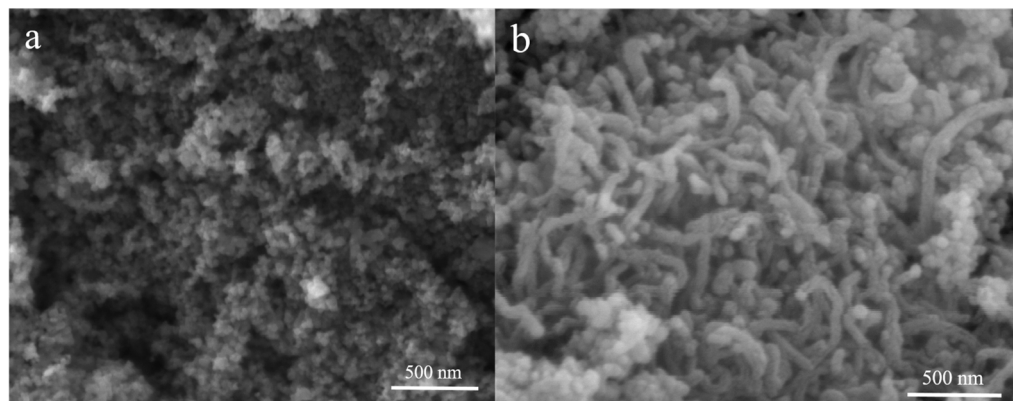


Figure 1. SEM micro-morphologies of the TiO_2 (a) and TiO_2/CNT (b) mesoporous nanomaterials.

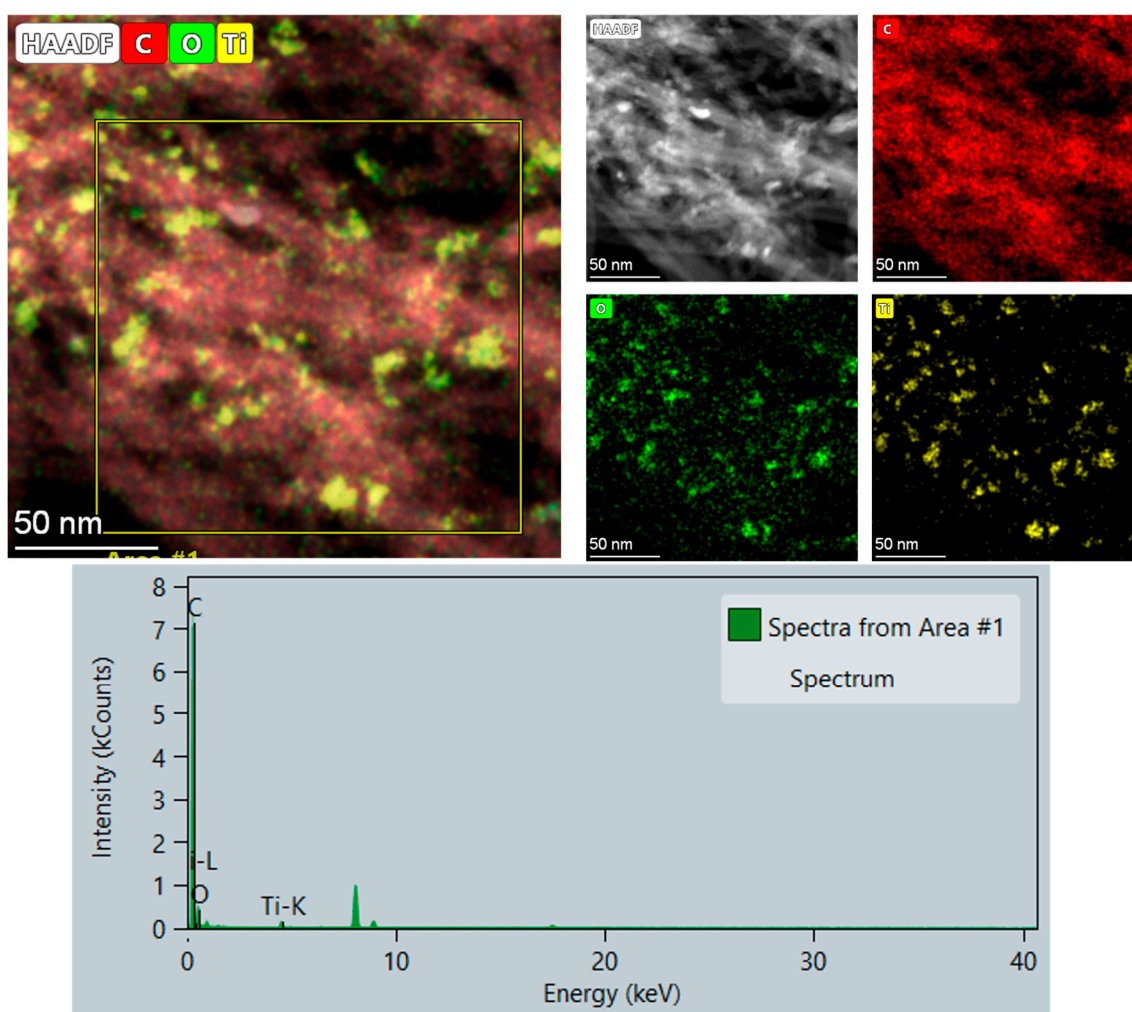


Figure 2. Energy-dispersive spectroscopy (EDS) mapping of the TiO_2/CNT mesoporous nanomaterials.

The microstructure of TiO_2 on CNTs was examined by TEM, which revealed different crystal planes of the composite (Figure 3a). After magnifying the red-circle area in Figure 3a,

more detailed information is presented in Figure 3b. The (101) interplanar spacing was 0.375 nm (Figure 3b), indicating that TiO₂ was an anatase phase [27,28], and the TiO₂ semiconductor composite on CNT improved the light absorption efficiency of the semiconductor composite [29].

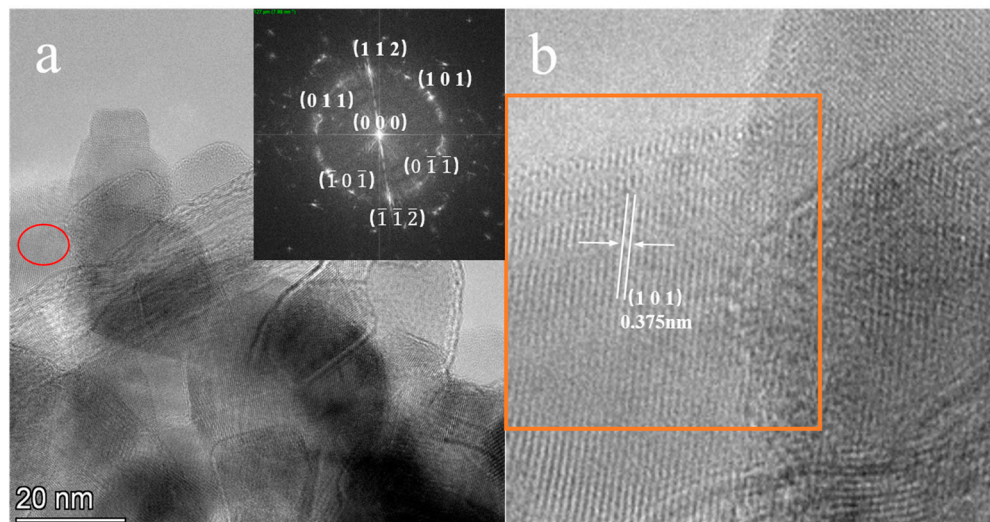


Figure 3. TEM (a) and high-resolution TEM (b) images of the TiO₂/CNT mesoporous nanomaterials.

According to the XRD results of the TiO₂/CNTs mesoporous composite (Figure 4a), the XRD PDF cards of TiO₂ and C were added for comparison. The TiO₂/CNT mesoporous composite was an obvious anatase phase and C phase, which was conducive to improving the photoelectric properties of the material [30–32]. This result corresponds with the observation in SEM and TEM. As shown in Figure 4b, the BET specific surface area of TiO₂/CNTs materials was 47.9 cm³/g, indicating the mesoporous structure. The high specific surface area was due to less agglomeration. When the relative pressure P/P_0 is between 0.4 and 1.0, there is a hysteric loop due to mesoporous adsorption, but the latter part of the curve bulged again, which corresponds to the porous adsorption system. Therefore, the dispersibility of TiO₂ on CNTs is good.

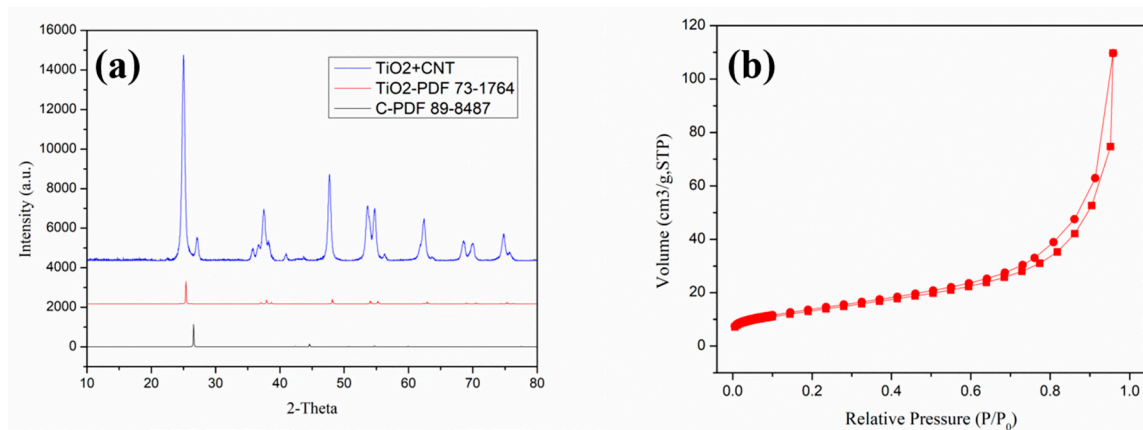


Figure 4. XRD pattern (a) and nitrogen adsorption–desorption isotherms (b) of the TiO₂/CNT mesoporous composite.

FT-IR was employed to analyze the functional groups on the film. The FTIR spectra in Figure 5 showed characteristic bands at 3400 cm⁻¹ and 1630 cm⁻¹ correspond to the surface water and hydroxyl group [33,34]. TiO₂ anatase has stable ultraviolet light absorption performance, but it has low light absorption efficiency in visible light and infrared light [35–37].

In order to improve the light absorption efficiency, carbon-doped TiO₂ nanomaterials were prepared [38,39]. It can be seen from Figure 5 that the infrared absorption efficiency of TiO₂/CNT mesoporous composite was higher than that of pure TiO₂, especially in the 600–800 nm band. Therefore, the carbon-doped TiO₂ nanomaterials behaved with a better light adsorption efficiency than the sample without carbon-doped TiO₂ nanomaterials.

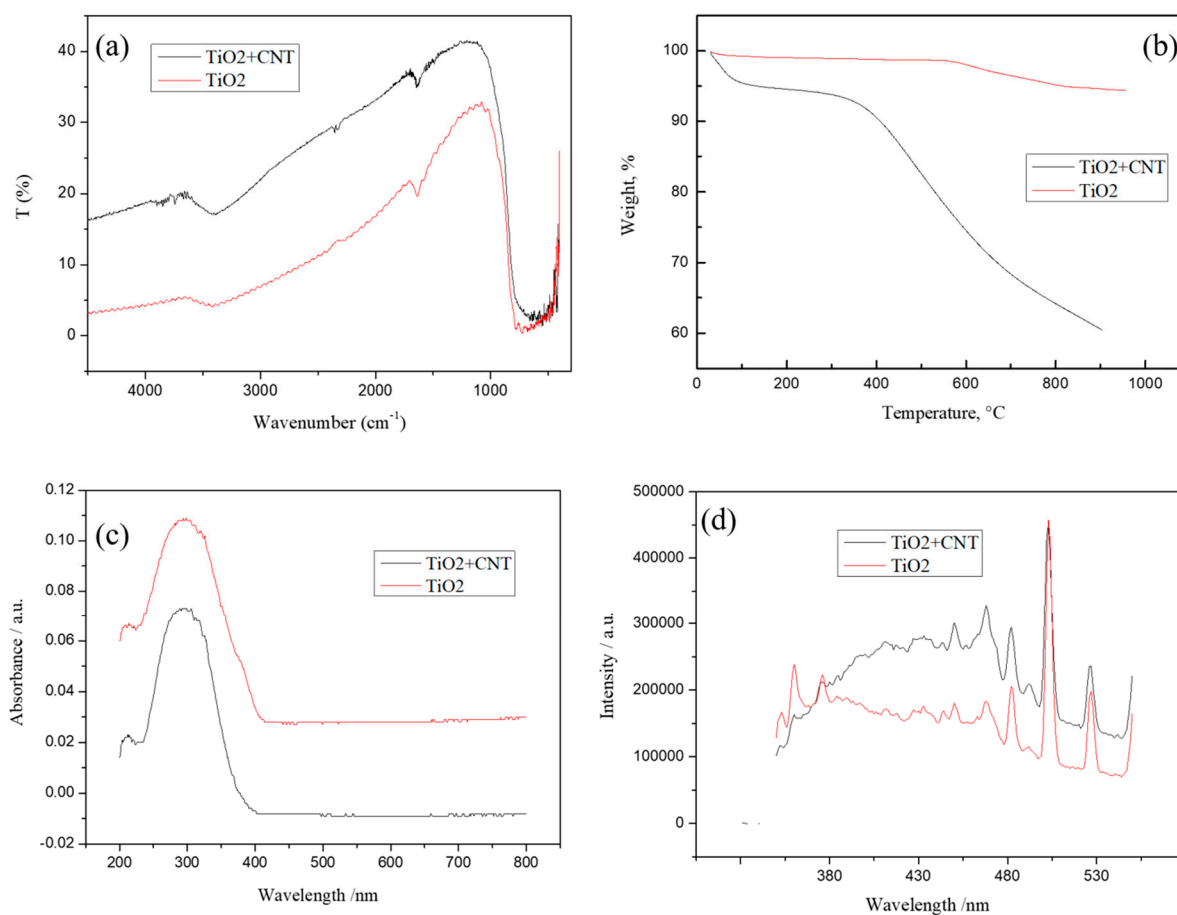


Figure 5. FT-IR spectra (a); thermogravimetric analysis (b); UV-vis (c) and photoluminescence spectra (d) of the TiO₂ + CNT mesoporous nanomaterials.

Biofouling including organic fouling on the conventional membrane surface is inevitable, which is caused by the nature of biological system, where microorganisms and bioparticles are the main components. The literature revealed that the structure/matrix of biofouling layer (biofilm) was highly related to the extracellular polymeric substances (EPS) compound. EPS is considered as the key component that determines the structural and functional integrity of microbial aggregates. It forms a three-dimensional, gel-like, highly hydrated and locally charged biofouling layer matrix, in which the microorganisms are more or less immobilized. In addition, EPS has also been reported to be the most significant foulant toward the conventional membrane fouling problems. Research has helped to address the problem, but it is still unclear what the major mechanism flaw is that causes biofouling, particularly on conventional membrane surfaces during the water treatment process. Currently, the industry practice to get rid of the biofilm is to take out the fouled membrane from the system and then soak it in chemicals such as sodium hypochlorite (NaOCl) and citric acid. This process causes three major problems: the generation of waste water, which requires further treatment; the interruption of the membrane treatment system, which reduces the production rate significantly; the reduction in membrane lifespan, which in turn increases the total cost of clean water production. The sterilization experiment embodies the photoelectric effect charge separation experiment. In order to test the visible light

absorption and bactericidal performance of TiO₂/CNT mesoporous composite, a mixture of *Escherichia coli* and different composites was made [40,41]. The mixture was spread on the agar medium after simulating sunlight irradiation, and the bactericidal results are shown in Figure 6. Figure 6(1) shows the blank group, and Figure 6(2) shows the bactericidal effect of TiO₂ mesoporous material. TiO₂ mesoporous material had a certain bactericidal effect, but TiO₂/CNT mesoporous nanomaterials (Figure 6(3)) had a stronger bactericidal effect. The main reason was that the absorption efficiency of visible light was improved after doping CNT, and the stable composite interface is prepared under a high-pressure hydrothermal environment. Therefore, according to the results of bactericidal experiments, the TiO₂/CNT mesoporous nanomaterials behaved with an excellent bactericidal performance, which is possible for clean industrial productions.

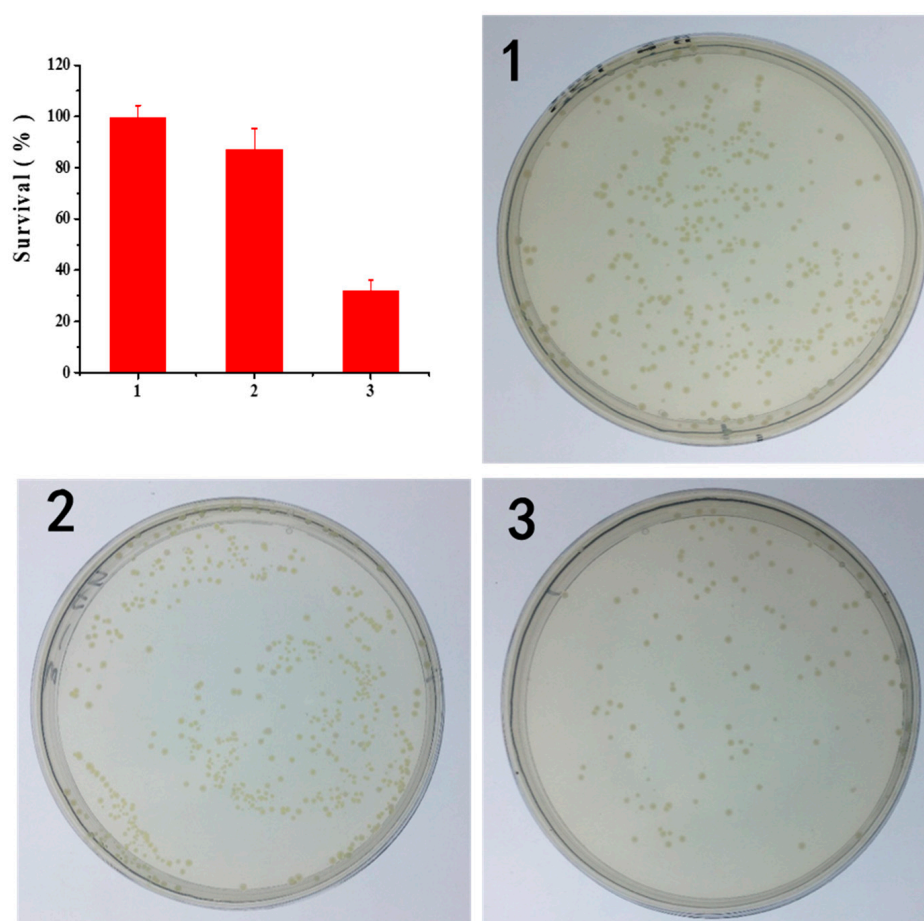


Figure 6. Bactericidal properties of the (1) black, (2) TiO₂ mesoporous material, and (3) TiO₂ + CNT mesoporous composite.

4. Conclusions

Preparation and stabilization of TiO₂/CNT nanocomposites at the composite interface by a high-pressure hydrothermal method. TiO₂/CNT mesoporous composite was prepared by the sol-gel method under an ultrasonic environment. Characterized under SEM and TEM, the composite materials contained TiO₂ nanoparticles as well as CNT. After phase analysis, it was the anatase-doped phase. Infrared absorption performance and *Escherichia coli* bactericidal performance tests under visible light showed that TiO₂/CNT mesoporous composite had better infrared and visible light absorption performance than pure TiO₂.

Author Contributions: Conceptualization, H.L. and Z.Z.; methodology, H.L. and Z.Z.; formal analysis, H.L. and Z.Z.; investigation, H.L. and Z.Z.; resources, H.L. and Z.Z.; data curation, H.L. and Z.Z.; writing—original draft preparation, H.L. and Z.Z.; writing—review and editing, W.Y., Y.L. and Z.F.; supervision, Y.L. and Z.F.; project administration, Y.L. and Z.F. All authors have read and agreed to the published version of the manuscript.

Funding: The authors received no external funding.

Institutional Review Board Statement: Not applicable.

Informed Consent Statement: Not applicable.

Data Availability Statement: Not applicable.

Conflicts of Interest: The authors declare no conflict of interest.

Sample Availability: Samples of the compounds are available from the authors.

References

1. Li, H.L.; Luo, S.W.; Zhang, L.Q.; Zhao, Z.L.; Wu, M.; Li, W.H.; Liu, F.Q. Water- and Acid-Sensitive Cu₂O@Cu-MOF Nano Sustained-Release Capsules with Superior Antifouling Behaviors. *ACS Appl. Mater. Interfaces* **2022**, *14*, 1910–1920. [[CrossRef](#)] [[PubMed](#)]
2. Pan, J.; Liu, G.; Lu, G.M.; Cheng, H.M. On the True Photoreactivity Order of {001}, {010}, and {101} Facets of Anatase TiO₂ Crystals. *Angew. Chem. Int. Edit.* **2011**, *50*, 2133–2137. [[CrossRef](#)] [[PubMed](#)]
3. Zhao, Z.L.; Li, H.L.; Huang, L.X.; Tan, Y.; Liu, F.Q.; Li, W.H. Preparation of graphene quantum dots-doped TiO₂ nanocomposites via a sol-gel method for photocathodic protection. *Mol. Cryst. Liq. Cryst.* **2021**, *731*, 80–87. [[CrossRef](#)]
4. Li, J.; Bai, H.; Feng, Z. Advances in the Modification of Silane-Based Sol-Gel Coating to Improve the Corrosion Resistance of Magnesium Alloys. *Molecules* **2023**, *28*, 2563. [[CrossRef](#)] [[PubMed](#)]
5. Geng, W.; Wang, L.; Yang, X.-Y. Nanocell hybrids for green chemistry. *Trends Biotechnol.* **2022**, *40*, 974–986. [[CrossRef](#)]
6. Zhao, Z.L.; Zhuang, Y.L.; Wang, T.; Zhao, D.S.; Wu, X. Influence of Al-Si eutectic alloy on the mechanical behaviors and microstructure feature of ultralight dual-phase Mg-8Li-x(Al-12.6 Si) alloys. *Mater. Today Commun.* **2022**, *30*, 103201. [[CrossRef](#)]
7. Zhao, Z.L.; Liu, Y.D.; Zhong, Y.F.; Chen, X.H.; Zhang, Z.Q. Corrosion Resistance of as-rolled Mg-Li-ALSi Alloys. *Int. J. Electrochem. Sci.* **2018**, *13*, 4338–4349. [[CrossRef](#)]
8. Zhao, Z.L.; Li, Y.H.; Zhong, Y.F.; Liu, Y.D. Corrosion Performance of as-rolled Mg-8Li-xAl Alloys. *Int. J. Electrochem. Sci.* **2019**, *14*, 6394–6405. [[CrossRef](#)]
9. Xue, S.-G.; Tang, L.; Tang, T.; Zhang, F.; Lyu, H.-G.; Liu, H.-Y.; Jiang, J.; Huang, Y.-H. Identifying the active sites in C-N codoped TiO₂ electrode for electrocatalytic water oxidation to produce H₂O₂. *J. Cent. South Univ.* **2022**, *29*, 3016–3029. [[CrossRef](#)]
10. Wang, Y.; Zhao, X.; Zheng, Z.; Jiang, H.; Chen, T.; Zhang, Y.; Cao, H.; Lin, H.; Zhan, R. Pd-M-TiO₂ (M=Mn, Cu, Ce and Fe) as passive NO_x adsorber (PNA) at low temperature. *J. Cent. South Univ.* **2022**, *29*, 2253–2265. [[CrossRef](#)]
11. Zada, A.; Ali, N.; Subhan, F.; Anwar, N.; Ali Shah, M.I.; Ateeq, M.; Hussain, Z.; Zaman, K.; Khan, M. Suitable energy platform significantly improves charge separation of g-C₃N₄ for CO₂ reduction and pollutant oxidation under visible-light. *Prog. Nat. Sci. Mater. Int.* **2019**, *29*, 138–144. [[CrossRef](#)]
12. Hao, D.; Liu, Y.; Gao, S.; Arandiyani, H.; Bai, X.; Kong, Q.; Wei, W.; Shen, P.K.; Ni, B.-J. Emerging artificial nitrogen cycle processes through novel electrochemical and photochemical synthesis. *Mater. Today* **2021**, *46*, 212–233. [[CrossRef](#)]
13. Rade, P.P.; Giram, P.S.; Shitole, A.A.; Sharma, N.; Garnaik, B. Physicochemical and in Vitro Antibacterial Evaluation of Metronidazole Loaded Eudragit S-100 Nanofibrous Mats for the Intestinal Drug Delivery. *Adv. Fiber Mater.* **2022**, *4*, 76–88. [[CrossRef](#)]
14. Wang, S.; Li, J.; Cao, Y.; Gu, J.; Wang, Y.; Chen, S. Non-Leaching, Rapid Bactericidal and Biocompatible Polyester Fabrics Finished with Benzophenone Terminated N-halamine. *Adv. Fiber Mater.* **2022**, *4*, 119–128. [[CrossRef](#)]
15. Du, Y.; Hao, Q.; Chen, D.; Chen, T.; Hao, S.; Yang, J.; Ding, H.; Yao, W.; Song, J. Facile fabrication of heterostructured bismuth titanate nanocomposites: The effects of composition and band gap structure on the photocatalytic activity performance. *Catal. Today* **2017**, *297*, 255–263. [[CrossRef](#)]
16. Tripathy, J.; Lee, K.; Schmuki, P. Tuning the Selectivity of Photocatalytic Synthetic Reactions Using Modified TiO₂ Nanotubes. *Angew. Chem. Int. Ed.* **2014**, *53*, 12605–12608. [[CrossRef](#)]
17. Lee, S.S.; Bai, H.; Liu, Z.; Sun, D.D. Novel-structured electrospun TiO₂/CuO composite nanofibers for high efficient photocatalytic cogeneration of clean water and energy from dye wastewater. *Water Res.* **2013**, *47*, 4059–4073. [[CrossRef](#)]
18. Tang, C.; Bai, H.; Liu, L.; Zan, X.; Gao, P.; Sun, D.D.; Yan, W. A green approach assembled multifunctional Ag/AgBr/TNF membrane for clean water production & disinfection of bacteria through utilizing visible light. *Appl. Catal. B Environ.* **2016**, *196*, 57–67. [[CrossRef](#)]
19. Zhao, Z.; Jiang, X.; Li, S.; Li, L.; Feng, Z.; Lai, H. Microstructure Characterization and Battery Performance Comparison of MOF-235 and TiO₂-P25 Materials. *Crystals* **2022**, *12*, 152. [[CrossRef](#)]
20. Zheng, H.; Guo, Y.-C.; Shen, F.-M. Production of titanium powder by metallothermic reduction of TiO₂ in cold pressed pellets. *J. Cent. South Univ.* **2021**, *28*, 48–57. [[CrossRef](#)]

21. Zouheir, M.; Tanji, K.; Navio, J.A.; Hidalgo, M.C.; Jaramillo-Páez, C.A.; Kherbeche, A. Effective photocatalytic conversion of formic acid using iron, copper and sulphate doped TiO₂. *J. Cent. South Univ.* **2022**, *29*, 3592–3607. [[CrossRef](#)]
22. Yang, F.; Wen, L.; Peng, Q.; Zhao, Y.; Xu, J.; Hu, M.; Zhang, S.; Yang, Z. Prediction of structural and electronic properties of Cl₂ adsorbed on TiO₂(100) surface with C or CO in fluidized chlorination process: A first-principles study. *J. Cent. South Univ.* **2021**, *28*, 29–38. [[CrossRef](#)]
23. Fan, B.; Liu, H.; Wang, Z.; Zhao, Y.; Yang, S.; Lyu, S.; Xing, A.; Zhang, J.; Li, H.; Liu, X. Ferroelectric polarization-enhanced photocatalytic performance of heterostructured BaTiO₃@TiO₂ via interface engineering. *J. Cent. South Univ.* **2021**, *28*, 3778–3789. [[CrossRef](#)]
24. Xiang, J.; Wang, S.C.; Cao, Y.X.; Fang, L.N.; Ke, W.; Guo, H.; Duan, B.Y.; Yu, W.H.; Li, L.; Zhao, Z.L. One-Step Preparation of High Performance TiO₂/CNT/CQD Nanocomposites Bactericidal Coating with Ultrasonic Radiation. *Coatings* **2023**, *13*, 145. [[CrossRef](#)]
25. Zhao, Z.; Lai, H.S.; Li, H.; Li, L. Preparation and Properties of Graphene Doped TiO₂ Mesoporous Materials for Photocathode Protection. *Int. J. Electrochem. Sci.* **2021**, *16*, 210316. [[CrossRef](#)]
26. Zada, A.; Khan, M.; Hussain, Z.; Shah, M.I.A.; Ateeq, M.; Ullah, M.; Ali, N.; Shaheen, S.; Yasmeen, H.; Ali Shah, S.N.; et al. Extended visible light driven photocatalytic hydrogen generation by electron induction from g-C₃N₄ nanosheets to ZnO through the proper heterojunction. *Z. Phys. Chem.* **2022**, *236*, 53–66. [[CrossRef](#)]
27. Wang, Y.X.; Rao, L.; Wang, P.F.; Shi, Z.Y.; Zhang, L.X. Photocatalytic activity of N-TiO₂/O-doped N vacancy g-C₃N₄ and the intermediates toxicity evaluation under tetracycline hydrochloride and Cr(VI) coexistence environment. *Appl. Catal. B Environ.* **2020**, *262*, 12. [[CrossRef](#)]
28. Wang, C.J.; Zhao, Y.L.; Xu, H.; Li, Y.F.; Wei, Y.C.; Liu, J.; Zhao, Z. Efficient Z-scheme photocatalysts of ultrathin g-C₃N₄-wrapped Au/TiO₂-nanocrystals for enhanced visible-light-driven conversion of CO₂ with H₂O. *Appl. Catal. B Environ.* **2020**, *263*, 13. [[CrossRef](#)]
29. Zhao, J.; Zhang, J.L.; Wang, L.; Lyu, S.S.; Ye, W.L.; Xu, B.B.; Qiu, H.; Chen, L.X.; Gu, J.W. Fabrication and investigation on ternary heterogeneous MWCNT@TiO₂-C fillers and their silicone rubber wave-absorbing composites. *Compos. Part. A Appl. Sci. Manuf.* **2020**, *129*, 8. [[CrossRef](#)]
30. Zhou, W.; Sun, F.; Pan, K.; Tian, G.; Jiang, B.; Ren, Z.; Tian, C.; Fu, H. Well-Ordered Large-Pore Mesoporous Anatase TiO₂ with Remarkably High Thermal Stability and Improved Crystallinity: Preparation, Characterization, and Photocatalytic Performance. *Adv. Funct. Mater.* **2011**, *21*, 1922–1930. [[CrossRef](#)]
31. Zhou, W.; Li, W.; Wang, J.-Q.; Qu, Y.; Yang, Y.; Xie, Y.; Zhang, K.; Wang, L.; Fu, H.; Zhao, D. Ordered Mesoporous Black TiO₂ as Highly Efficient Hydrogen Evolution Photocatalyst. *J. Am. Chem. Soc.* **2014**, *136*, 9280–9283. [[CrossRef](#)]
32. Xu, H.M.; Liu, W.; Cao, L.X.; Su, G.; Duan, R.J. Preparation of porous TiO₂/ZnO composite film and its photocathodic protection properties for 304 stainless steel. *Appl. Surf. Sci.* **2014**, *301*, 508–514. [[CrossRef](#)]
33. Hu, G.; Xiao, Y.; Ying, J. Nano-SiO₂ and Silane Coupling Agent Co-Decorated Graphene Oxides with Enhanced Anti-Corrosion Performance of Epoxy Composite Coatings. *Int. J. Mol. Sci.* **2021**, *22*, 11087. [[CrossRef](#)]
34. Li, J.; Li, T.; Zeng, Y.; Chen, C.; Guo, H.; Lei, B.; Zhang, P.; Feng, Z.; Meng, G. A novel sol-gel coating via catechol/lysine polymerization for long-lasting corrosion protection of Mg alloy AZ31. *Colloids Surf. A Physicochem. Eng. Asp.* **2023**, *656*, 130361. [[CrossRef](#)]
35. Ghicov, A.; Albu, S.P.; Hahn, R.; Kim, D.; Stergiopoulos, T.; Kunze, J.; Schiller, C.-A.; Falaras, P.; Schmuki, P. TiO₂ Nanotubes in Dye-Sensitized Solar Cells: Critical Factors for the Conversion Efficiency. *Chem. Asian J.* **2009**, *4*, 520–525. [[CrossRef](#)]
36. Lu, Y.; Cheng, X.; Tian, G.; Zhao, H.; He, L.; Hu, J.; Wu, S.-M.; Dong, Y.; Chang, G.-G.; Lenaerts, S.; et al. Hierarchical CdS/m-TiO₂/G ternary photocatalyst for highly active visible light-induced hydrogen production from water splitting with high stability. *Nano Energy* **2018**, *47*, 8–17. [[CrossRef](#)]
37. Nie, X.; Yin, S.; Duan, W.; Zhao, Z.; Li, L.; Zhang, Z. Recent Progress in Anodic Oxidation of TiO₂ Nanotubes and Enhanced Photocatalytic Performance: A Short Review. *Nano* **2021**, *16*, 2130002. [[CrossRef](#)]
38. Asahi, R.; Morikawa, T.; Ohwaki, T.; Aoki, K.; Taga, Y. Visible-light photocatalysis in nitrogen-doped titanium oxides. *Science* **2001**, *293*, 269–271. [[CrossRef](#)]
39. Zheng, J.Y.; Lyu, Y.H.; Wang, R.L.; Xie, C.; Zhou, H.J.; Jiang, S.P.; Wang, S.Y. Crystalline TiO₂ protective layer with graded oxygen defects for efficient and stable silicon-based photocathode. *Nat. Commun.* **2018**, *9*, 3572. [[CrossRef](#)]
40. Wu, Q.; Liu, X.M.; Li, B.; Tan, L.; Han, Y.; Li, Z.Y.; Liang, Y.Q.; Cui, Z.D.; Zhu, S.L.; Wu, S.L.; et al. Eco-friendly and degradable red phosphorus nanoparticles for rapid microbial sterilization under visible light. *J. Mater. Sci. Technol.* **2021**, *67*, 70–79. [[CrossRef](#)]
41. Avsec, K.; Conradi, M.; Jenko, M.; Kocjancic, B.; Debeljak, M.; Gorenssek, M.; Dolinar, D. Effect of sterilization on the surface properties of ti6al7nb alloy femoral stems. *Mater. Tehnol.* **2021**, *55*, 59–64. [[CrossRef](#)]

Disclaimer/Publisher’s Note: The statements, opinions and data contained in all publications are solely those of the individual author(s) and contributor(s) and not of MDPI and/or the editor(s). MDPI and/or the editor(s) disclaim responsibility for any injury to people or property resulting from any ideas, methods, instructions or products referred to in the content.